



Application of statistical physics to heartbeat diagnosis

S. Havlin^{a,b,*}, L.A.N. Amaral^b, Y. Ashkenazy^a, A.L. Goldberger^c,
P.Ch. Ivanov^{b,c}, C.-K. Peng^{b,c}, H.E. Stanley^b

^a*Gonda-Goldschmied Center, Department of Physics, Bar-Ilan University, Ramat-Gan 52900, Israel*

^b*Center for Polymer Studies and Department of Physics, Boston University, Boston, MA 02215, USA*

^c*Cardiovascular Division, Harvard Medical School, Beth Israel Hospital, Boston, MA 02215, USA*

Abstract

We present several recent studies based on statistical physics concepts that can be used as diagnostic tools for heart failure. We describe the scaling exponent characterizing the long-range correlations in heartbeat time series as well as the multifractal features recently discovered in heartbeat rhythm. It is found that both features, the long-range correlations and the multifractality, are weaker in cases of heart failure. © 1999 Elsevier Science B.V. All rights reserved.

1. The human heartbeat

It is common to describe the normal electrical activity of the heart as “regular sinus rhythm”. However, cardiac interbeat intervals fluctuate in a complex, apparently erratic manner in healthy subjects even at rest. Analysis of heart rate variability has focused primarily on short time oscillations associated with breathing (0.15–0.40 Hz) and blood pressure control (~ 0.1 Hz) [1]. Fourier analysis of longer heart-rate sets from healthy individuals typically reveals a $1/f$ -like spectrum for frequencies < 0.1 Hz [2–7].

Peng et al. [8–10] studied scale-invariant properties of the human heartbeat time series. The analysis is based on beat-to-beat heart rate fluctuations over very long time intervals (up to 24 h $\approx 10^5$ beats) recorded with an ambulatory monitor.¹ The time

* Correspondence address: Gonda-Goldschmied Center, Department of Physics, Bar-Ilan University, Ramat-Gan 52900, Israel. Fax: +972-3-535-3298.

E-mail address: havlin@phys9.ph.biu.ac.il (S. Havlin)

¹ Heart Failure Database (Beth Israel Deaconess Medical Center, Boston, MA). The database includes 18 healthy subjects (13 female and 5 male, with ages between 20 and 50, average 34.3 yr), and 12 congestive heart failure subjects (3 female and 9 male, with ages between 22 and 71, average 60.8 yr) in sinus rhythm.

series obtained by plotting the sequential intervals between beat n and beat $n + 1$, denoted by $B(n)$, typically reveals a complex type of variability. This variability is related to competing neuroautonomic inputs.

To study these dynamics over large time scales, the time series is passed through a digital filter that removes fluctuations of frequencies $> 0.005 \text{ beat}^{-1}$. We plot the result, denoted by $B_L(n)$, in Fig. 1. One observes a more complex pattern of fluctuations for a representative healthy adult (Fig. 1a) compared to the “smoother” pattern of interbeat intervals for a subject with severe heart disease (Fig. 1b). These heartbeat time series produce a contour reminiscent of the irregular landscapes that have been widely studied in physical systems.

To quantitatively characterize such a “landscape”, Peng et al. [8–10] study a mean fluctuation function $F(n)$, defined as

$$F(n) \equiv \overline{|B(n' + n) - B(n')|}, \quad (1)$$

where the bar denotes an average over all values of n' . Since $F(n)$ measures the average difference between two interbeat intervals separated by a time lag n , $F(n)$ quantifies the magnitude of the fluctuations over different time scales n .

Fig. 1c is a log–log plot of $F(n)$ vs. n for the data in Figs. 1a and b. This plot is approximately linear over a broad physiologically relevant time scale (200–4000 beats) implying that

$$F(n) \sim n^\alpha. \quad (2)$$

It is found that the scaling exponent α is markedly different for the healthy and diseased states: for the healthy heartbeat data, α is close to 0, while α is close to 0.5 for the diseased case. Note that $\alpha = 0.5$ corresponds to a random walk (a Brownian motion), thus the low-frequency heartbeat fluctuations for a diseased state can be interpreted as a stochastic process, in which the interbeat intervals $I(n) \equiv B(n + 1) - B(n)$ are uncorrelated for $n \geq 200$.

To investigate these dynamical differences, it is helpful to study further the correlation properties of the time series. Since $I(n)$ is more stationary, one can apply standard spectral analysis techniques [13,14]. The power spectra $S_I(f)$, the square of the Fourier transform amplitudes for $I(n)$, yields

$$S_I(f) \sim \frac{1}{f^\beta}. \quad (3)$$

The exponent β is related to α by $\beta = 2\alpha - 1$ [15]. Furthermore, β can serve as an indicator of the presence and type of correlations:

- (i) If $\beta = 0$, there is no correlation in the time series $I(n)$ (“white noise”).
- (ii) If $0 < \beta < 1$, then $I(n)$ is correlated such that positive values of I are likely to be close (in time) to each other, and the same is true for negative I values.
- (iii) If $-1 < \beta < 0$, then $I(n)$ is also correlated; however, the values of I are organized such that positive and negative values are more likely to alternate in time (“anti-correlation”).

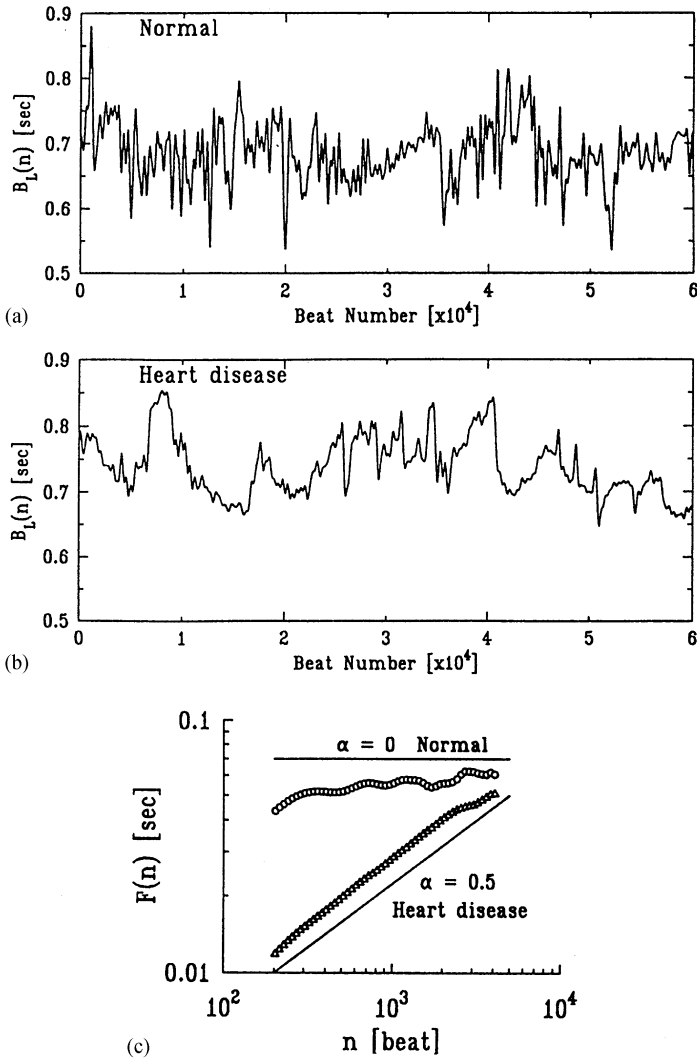


Fig. 1. The interbeat interval $B_L(n)$ after low-pass filtering for (a) a healthy subject and (b) a patient with severe cardiac disease (dilated cardiomyopathy). The healthy heartbeat time series shows more complex fluctuations compared to the diseased heart rate fluctuation pattern that is close to random walk (“brown”) noise. (c) Log–log plot of $F(n)$ vs. n . The circles represent $F(n)$ calculated from data in (a) and the triangles from data in (b). The two best-fit lines have slope $\alpha = 0.07$ and $\alpha = 0.49$ (fit from 200 to 4000 beats). The two lines with slopes $\alpha = 0$ and $\alpha = 0.5$ correspond to “ $1/f$ noise” and “brown noise”, respectively. We observe that $F(n)$ saturates for large n (of the order of 5000 beats), because the heartbeat interval are subjected to physiological constraints that cannot be arbitrarily large or small. After Peng et al. [8–10].

For the diseased data set, we observe a flat spectrum ($\beta \approx 0$) in the low-frequency region confirming that $I(n)$ are not correlated over long time scales (low frequencies). In contrast, for the data set from the healthy subject we obtain $\beta \approx -1$, indicating *nontrivial* long-range correlations in $B(n)$ – these correlations are not the consequence

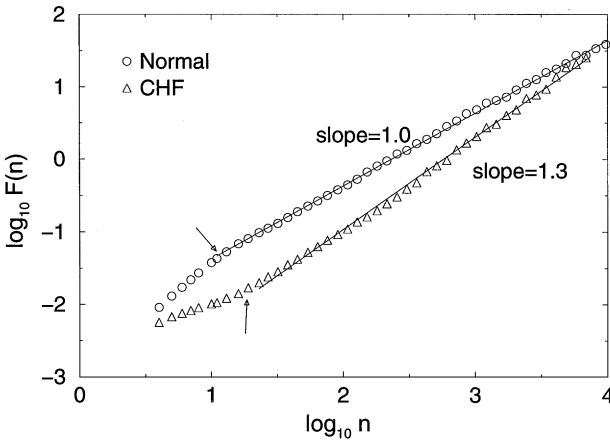


Fig. 2. Plot of $\log F(n)$ vs. $\log n$ for two long interbeat interval time series (~ 24 h). The circles are for a representative healthy subject while the triangles are from a subject with congestive heart failure. Arrows indicate “crossover” points in scaling. Note altered scaling with heart failure, suggesting apparent perturbations of both short and long-range correlation mechanisms. After Peng et al. [8–10].

of summation over random variables or artifacts of non-stationarity. Furthermore, the “anti-correlation” properties of $I(n)$ indicated by the negative β value are consistent with a nonlinear feed-back system that “kicks” the heart rate away from extremes. This tendency, however, does not only operate on a beat-to-beat basis (local effect) but on a wide range of time scales.

A further improvement to the study of the long-range correlation exponent α – detrended fluctuation analysis (DFA) – has been proposed and developed by Peng et al. [11,12]. Fig. 2 compares the DFA analysis of representative 24 h interbeat interval time series of a healthy subject (\circ) and a patient with congestive heart failure (\triangle). Note that for large time scales (asymptotic behavior), the healthy subject shows almost perfect power-law scaling over more than two decades ($20 \leq n \leq 10\,000$) with $\alpha_{\text{DFA}} = 1$ (i.e., $1/f$ noise) while for the pathologic data set $\alpha_{\text{DFA}} \approx 1.3$ (closer to Brownian noise). This result is consistent with our previous finding [8–10] that there is a significant difference in the long-range scaling behavior between healthy and diseased states.

To study the alteration of long-range correlations with pathology, we analyzed cardiac interbeat data from three different groups of subjects: (i) 29 adults (17 male and 12 female) without clinical evidence of heart disease (age range: 20–64 yr, mean 41), (ii) 10 subjects with fatal or near-fatal sudden cardiac death syndrome (age range: 35–82 yr) and (iii) 15 adults with severe heart failure (age range: 22–71 yr; mean 56). Data from each subject contains approximately 24 h of ECG recording encompassing $\sim 10^5$ heartbeats.

For the normal control group, we observed $\alpha_{\text{DFA}} = 1.00 \pm 0.10$ (mean value \pm S.D.). These results indicate that healthy heart rate fluctuations are anticorrelated and exhibit

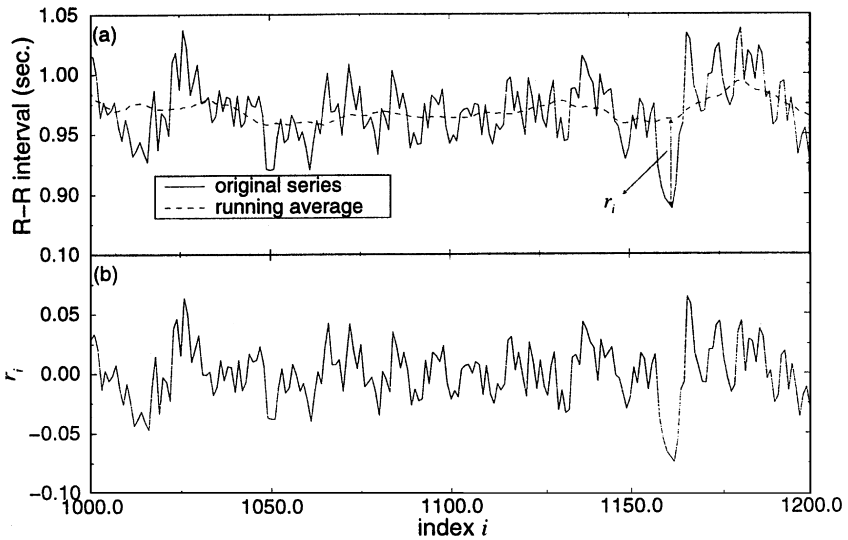


Fig. 3. (a) Segment of RR-interval data vs. beat number (solid curve) and running average based on a local window of 32 heart beats (dashed curve). (b) Detrended curve, i.e., the difference between solid curve and broken curve in top panel. After Askenazy et al. [16].

long-range power-law (fractal) correlation behavior over three decades. Furthermore both pathologic groups show significant deviation of the long-range correlations exponent α_{DFA} from the normal value $\alpha_{\text{DFA}} = 1$. For the group of heart failure subjects, we find that $\alpha_{\text{DFA}} = 1.24 \pm 0.22$, while for the group of sudden cardiac death syndrome subjects, we find that $\alpha_{\text{DFA}} = 1.22 \pm 0.25$.

The different scaling behavior in health and disease must relate to the underlying dynamics of the heartbeat. Applications of this analysis may lead to new diagnostics for patients at high risk of cardiac disease and sudden death.

2. The detrended time series

In this section we present a method of detrending a times series in the following way. First, from the time-series of the raw $B(n) \equiv RR$ data a running average is constructed using an interval-length of 2^m . Next, the running average is subtracted from the original RR-data time series. This procedure is illustrated in Fig. 3a, where the solid curve represents the raw RR-data and the dashed curve represents the running average. The difference between the two curves is denoted by r_i and is shown in Fig. 3b. The resultant time-series r_i is called the detrended time series (DTS) [16] and represents the fluctuations with respect to the local average. This procedure partly removes noise and slow oscillations which should not directly affect the short time scales in the time series [17,18].

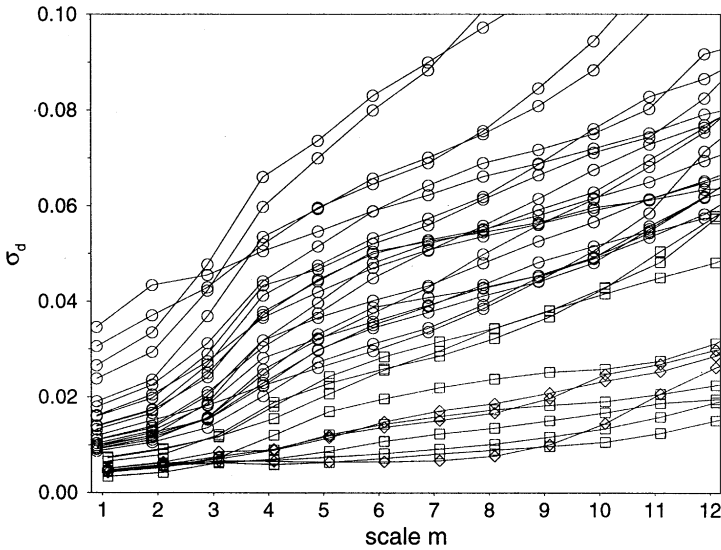


Fig. 4. Standard deviation (in seconds) of the detrended series for a group of 33 subjects vs. the scale factor of the local window used in the detrending. Healthy subjects: Circles, Diabetics: Squares and Heart patients: Rhombhedra. The three topmost diabetics can be regarded clinically as healthy. After Ashkenazy et al. [16].

The standard deviation σ_d of the DTS, using a detrending window of scale m , includes only the behavior of relevant small time scales and may thus be considered a measure of the heart rate variability. To evaluate the discriminating capabilities of σ_d , RR-data for a group of 33 subjects (the same data group as in ref. [19] consisting of 21 healthy subjects, 9 diabetics and 3 heart patients including one heart-transplant patient) were examined [16]. Using a time-series consisting of $2^{16} = 65536$ data points, corresponding to 16 hours of measured ECG data, and for the scale values $m = 1-12$ for the detrending window σ_d is calculated. The smallest detrending window is thus 2 and the largest 4096. Results are shown in Fig. 4, which is the analogous of Fig. 4 in Ref. [19] and Fig. 1 in Ref. [20]. In Fig. 4 one notes a clear separation between the group of healthy subjects (circles) on the one hand, and the groups of diabetics (squares) and heart patients (rhombhedra) on the other hand. However, one also notes from this figure that 3 of the diabetics (the three topmost) with as much justification could have been included in the group of healthy subjects thus displacing the separation region for σ_d towards lower values.

In Fig. 4 the largest separation between the healthy subjects and the two other groups is found for the scale $m=8-11$, whereas for an alternative analysis the largest separation was found for the scale $m=4-6$ [19,20]. Indeed, such a separation was earlier identified by Peng et al. [21] (see Fig. 2). Ref. [22] discusses the scale dependence of the different methods. The DFA analysis yields a crossover point for the fractal slope for the scale $m=4$ [21,22]. It should be noted, however, that the crossover point in the DFA analysis

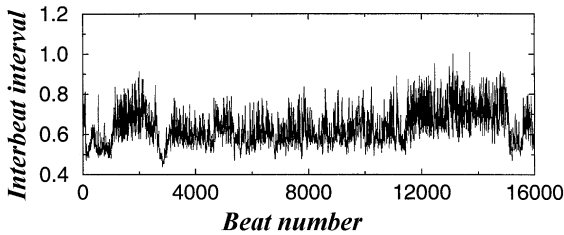


Fig. 5. Consecutive heartbeat intervals measured in seconds are plotted vs. beat number from approximately 3 hrs record of a representative healthy subject. The time series exhibits very irregular and nonstationary behavior.

is not a sharply defined point, rather the change in fractal slope takes place in a gradual way.

3. Multifractality in human heartbeat dynamics

In view of the heterogeneous (“patchy”) nature of the heartbeat interval time series (Fig. 5), it has been suggested by Ivanov et al. [23] that a single exponent is not sufficient to characterize the complexity of the cardiac dynamics, and that a multifractal approach may be necessary [24,25]. To test the hypothesis that an infinite number of exponents is required to characterize healthy dynamics [23], a multifractal analysis of heartbeat interval time series has been performed and $D(h)$ has been calculated using wavelet methods [26].

The properties of the wavelet transform make wavelet methods attractive for the analysis of complex nonstationary time series such as one encounters in physiological signals. In particular, wavelets can remove polynomial trends that could lead box-counting techniques to fail to quantify the local scaling of the signal [27]. Additionally, the time–frequency localization properties of the wavelets makes them particularly useful for the task of revealing the underlying hierarchy that governs the temporal distribution of the local Hurst exponents [15,28]. Hence, the wavelet transform enables a reliable multifractal analysis [27,28].

As the analyzing wavelet, we use n -order derivatives of the Gaussian function. Such a wavelet allows us to estimate the singular behavior and the corresponding exponent h at a given location in the time series. The higher the order n of the derivative, the higher the order of the polynomial trends removed and the better the detection of the temporal structure of the local scaling exponents in the signal.

We extract the local value of h through the modulus of the maxima values of the wavelet transform at each point in the time series. We then estimate the scaling of the partition function $Z_q(a)$, which is defined as the sum of the q th powers of the local maxima of the modulus of the wavelet transform coefficients at scale a [28]. For small scales, we expect

$$Z_q(a) \sim a^{\tau(q)}. \quad (4)$$

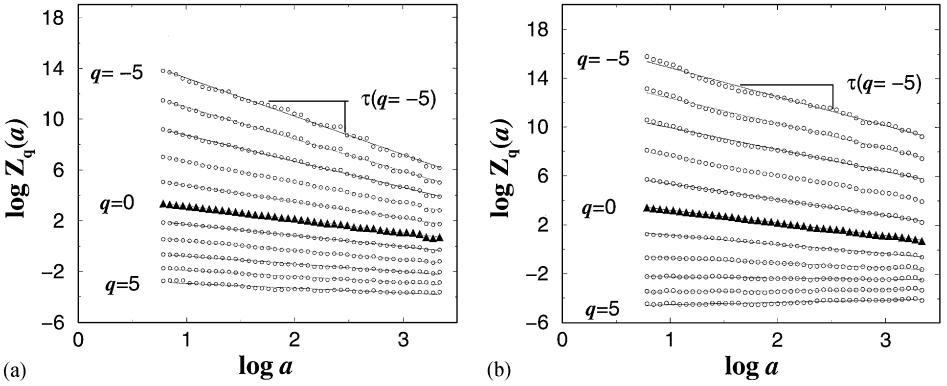


Fig. 6. Heartbeat time series contain densely packed, *non-isolated* singularities which unavoidably affect each other in the time–frequency decomposition. Therefore, rather than evaluating the distribution of the inherently unstable local singularity exponents, we estimate the scaling of an appropriately chosen global measure: the q moments of the probability distribution of the maxima of the wavelet transform $Z_q(a)$ (as analyzing wavelet we use the 3rd derivative of the Gaussian function). Here we show the scaling of the partition function $Z_q(a)$ with scale a obtained from daytime records consisting of $\approx 25,000$ beats for (a) a healthy subject and (b) a subject with congestive heart failure. We calculate $\tau(q)$ for moments $q = -5, 4, \dots, 0, \dots, 5$ and scales $a = 2 \times 1.15^i$, $i = 0, \dots, 41$. We display the calculated values for $Z_q(a)$ for scales $a > 8$. The top curve corresponds to $q = -5$, the middle curve (shown heavy) to $q = 0$ and the bottom curve to $q = 5$. The exponents $\tau(q)$ are obtained from the slope of the curves in the region $16 < a < 700$, thus eliminating the influence of any residual small scale random noise due to ECG signal pre-processing as well as extreme, large scale fluctuations of the signal. After Ivanov et al. [23].

For certain values of q , the exponents $\tau(q)$ are related to other familiar exponents. In particular, $\tau(2)$ is related to the scaling exponent of the Fourier power spectra, $S(f) \sim 1/f^{-\beta}$, as $\beta = 2 + \tau(2)$. For positive q , $Z_q(a)$ reflects the scaling of the large fluctuations and strong singularities, while for negative q , $Z_q(a)$ reflects the scaling of the small fluctuations and weak singularities. Thus, the scaling exponents $\tau(q)$ can reveal different aspects of cardiac dynamics.

We define the fractal dimensions $D(h)$ through a Legendre transform of $\tau(q)$ [15],

$$D(h) = qh(q) - \tau(q), \quad h(q) \equiv \frac{d\tau(q)}{dq}. \quad (5)$$

Monofractals display a linear $\tau(q)$ spectrum, $\tau(q) = qH - 1$, where H is the global Hurst exponent. For multifractal signals $\tau(q)$ is a nonlinear function: $\tau(q) = qh(q) - 1$, where $h(q)$ is not constant.

We analyze both diurnal (12:00 to 18:00) and nocturnal (0:00 to 6:00) heartbeat time series records of 18 healthy subjects, and the diurnal records of 12 patients with congestive heart failure. For all subjects, we find that for a broad range of positive and negative q the partition function $Z_q(a)$ scales as a power law (Figs. 6a and b). In Fig. 7, we show $Z_q(a)$ for $q = -2$ and 2 for all 18 healthy subjects in our database. This figure shows that there is good power-law scaling – that is, the data points fall on a straight line in a log–log plot – for all subjects and across nearly two orders of magnitude in a . Also, it is clear that the data have nearly the same slope for all

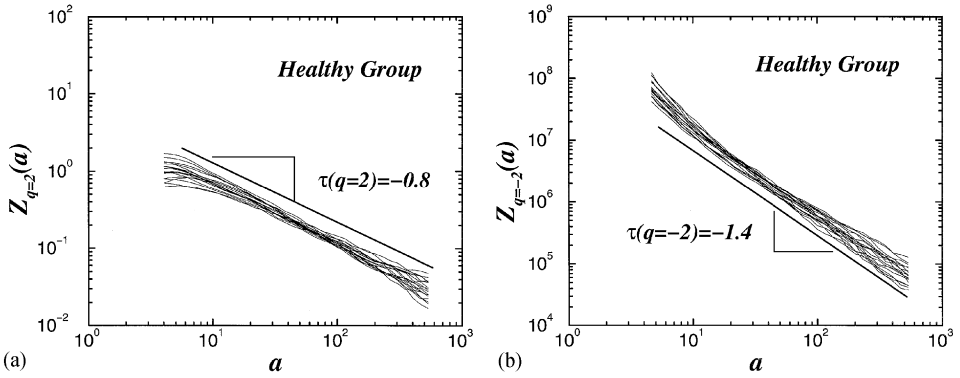


Fig. 7. Scaling of $Z_q(a)$ for the entire healthy group for $q = 2$ and $q = -2$. Courtesy of P.Ch. Ivanov.

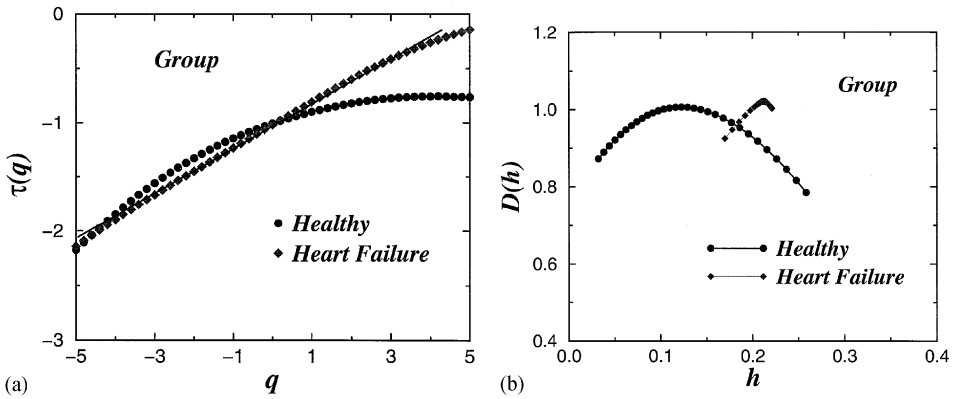


Fig. 8. (a) Multifractal spectrum $\tau(q)$ of the group averages for daytime and night time records for 18 healthy subjects and for 12 patients with congestive heart failure. The results show multifractal behavior for the healthy group and distinct change in this behavior for the heart failure group. (b) Fractal dimensions $D(h)$ obtained through a Legendre transform from the group averaged $\tau(q)$ spectra of (a). The shape of $D(h)$ for the individual records and for the group average is broad, indicating multifractal behavior. On the other hand, $D(h)$ for the heart failure group is very narrow, indicating monofractality. The different form of $D(h)$ for the heart failure group may reflect perturbation of the cardiac neuroautonomic control mechanisms associated with this pathology. After Ivanov et al. [23].

subjects. The exponent of the DFA is $\alpha_{\text{DFA}} = [\tau(r) + 3]/2$ [11,12]. This result yields $\alpha_{\text{DFA}} \approx 1.1$ for healthy records and a similar analysis yields $\alpha_{\text{DFA}} \approx 1.3$ for congestive heart failure in agreement with [21].

For all healthy subjects, we find that $\tau(q)$ is a nonlinear function (Figs. 8a), which indicates that the heart rate of healthy humans is a multifractal signal. Fig. 8b shows that for healthy subjects, $D(h)$ has nonzero values for a broad range of local Hurst exponents h . The multifractality of healthy heartbeat dynamics cannot be explained by activity, as we analyze data from subjects during nocturnal hours. Furthermore, this multifractal behavior cannot be attributed to sleep stage transition, as we find

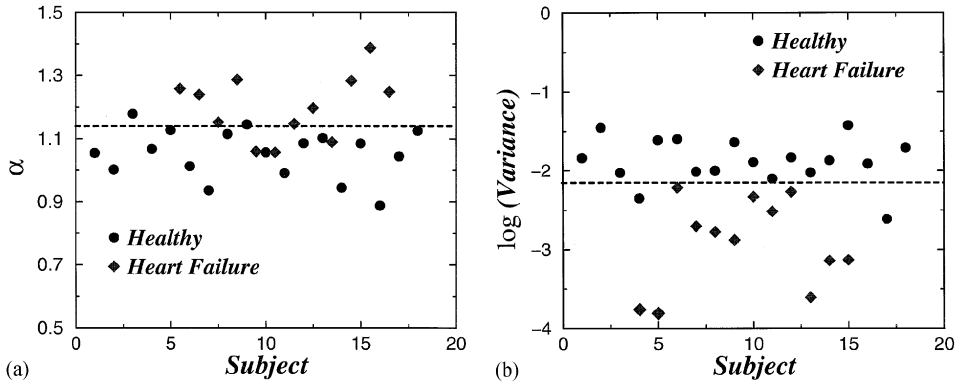


Fig. 9. (a) Correlation exponent and (b) variance of wavelet coefficients. Courtesy of P.Ch. Ivanov and L.A.N. Amaral.

multifractal features during daytime hours as well. The range of scaling exponents— $0 < h < 0.4$ —with nonzero fractal dimension $D(h)$, suggests that the fluctuations in the healthy heartbeat dynamics exhibit strongly anti-correlated behavior (as opposed to $h = \frac{1}{2}$, which corresponds to uncorrelated behavior).

In contrast, subjects with a pathological condition—congestive heart failure—show a loss of multifractality (Figs. 8a and b). We find for the heart failure subjects that $D(h)$ is supported only over a narrow range of exponents h , which indicates weaker multifractality or even monofractality. Moreover, even when the same exponent h is present for both healthy and heart failure subjects, the fractal dimension $D(h)$ associated with this particular exponent has a smaller value for the heart failure subjects (Fig. 8).

Our results show that, for healthy subjects, local Hurst exponents in the range $0.1 < h < 0.2$ are associated with fractal dimensions close to one. This means that the subsets characterized by these local exponents are statistically dominant. On the other hand, for the heart failure subjects, we find that the statistically dominant exponents are confined to a narrow range of local Hurst exponents: $h \approx 0.3$. These results suggest that for heart failure the fluctuations are less anti-correlated than for healthy dynamics, since the dominant scaling exponents h are closer to $\frac{1}{2}$. Our findings support previous reports on long-range anti-correlations of heart beat intervals [21], and can be used as an alternative diagnostic tool.

We compare our method with other widely used methods of heart rate time series analysis. As an example, we show in Fig. 9 two well-established methods. The first is based on the measurement of long-range correlations on the fluctuations in heartbeat intervals [8–10]. These correlations have been quantified with both the power spectrum and the detrended fluctuation analysis. Fig. 9(a) shows the values of the correlation exponent α measured through the detrended fluctuation analysis. The dashed line represents an in-sample threshold for discrimination of the healthy and heart failure groups.

A second method based on Ref. [21] and recently applied in Refs. [16,20] measures the variance of the coefficients of the wavelet transform of the heartbeat signal at a

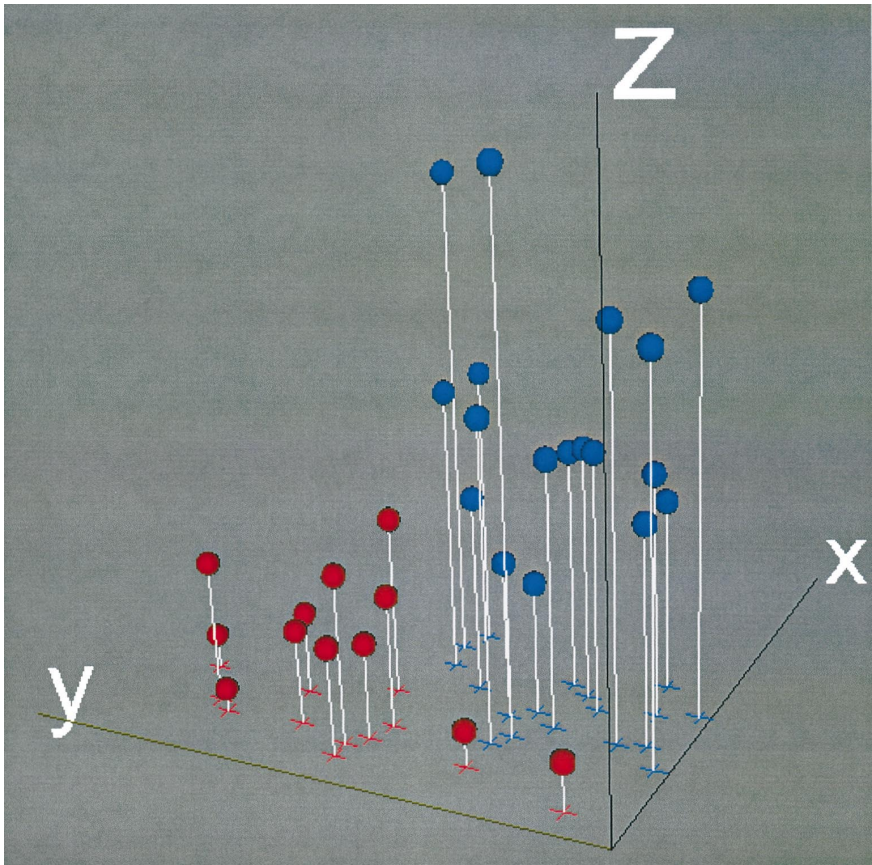


Fig. 10. A 3-D plot revealing the discriminating power of the multifractal approach. After Ivanov et al. [23].

wavelet scale of $a = 32$, shown in Fig. 9(b). The dashed line represents an in-sample threshold for discrimination of the healthy and heart failure groups. These two methods do not result in a fully consistent assignment, e.g., two heart failure subjects are assigned to the diseased group by the first method and to the healthy group by the second method.

Results of the multifractal method [23] are shown in Fig. 10. Each subject's dataset is characterized by three quantities. The first quantity (z -axis) is the degree of multifractality which is the difference between the maximum and minimum values of local Hurst exponent h for each individual [Fig. 8(b)]. Note that the degree of multifractality takes value zero for a monofractal.

The second quantity (y -axis) is the exponent value $\tau(q = 3)$ obtained from the scaling of the third moment $Z_3(a)$. The third quantity (x -axis) is the standard deviation of the interbeat intervals. The healthy subjects are represented with blue balls and the heart failure subjects in red. We see from Fig. 10 that the multifractal approach has the potential to robustly discriminate the healthy subjects from heart failure subjects.

Acknowledgement

Supported by the NIH/National Center for Research Resources (grant P41 13622).

References

- [1] W.F. Doolittle, in: E. Stone, R. Schwartz (Eds.), *Intervening Sequences in Evolution and Development*, Oxford University Press, New York, 1990, p. 42.
- [2] R.I. Kitney, O. Rompelman, *The Study of Heart-Rate Variability*, Oxford University Press, London, 1980.
- [3] S. Akselrod, D. Gordon, F.A. Ubel, D.C. Shannon, A.C. Barger, R.J. Cohen, *Science* 213 (1981) 220.
- [4] M. Kobayashi, T. Musha, *IEEE Trans. Biomed. Eng.* 29 (1982) 456.
- [5] A.L. Goldberger, D.R. Rigney, J. Mietus, E.M. Antman, S. Greenwald, *Experientia* 44 (1988) 983.
- [6] J.P. Saul, P. Albrecht, D. Berger, R.J. Cohen, *Computers in Cardiology*, IEEE Computers Society Press, Washington DC, 1987, pp. 419–422.
- [7] D.T. Kaplan, M. Talajic, *Chaos* 1 (1991) 251.
- [8] C.-K. Peng, J.E. Mietus, J.M. Hausdorff, S. Havlin, H.E. Stanley, A.L. Goldberger, *Phys. Rev. Lett.* 70 (1993) 1343.
- [9] C.-K. Peng, Ph.D. Thesis, Boston University, 1993.
- [10] C.-K. Peng, S.V. Buldyrev, J.M. Hausdorff, S. Havlin, J.E. Mietus, M. Simons, H.E. Stanley, A.L. Goldberger, in: G.A. Losa, T.F. Nonnenmacher, E.R. Weibel (Eds.), *Fractals in Biology and Medicine*, Birkhauser Verlag, Boston, 1994.
- [11] C.-K. Peng, S.V. Buldyrev, S. Havlin, M. Simons, H.E. Stanley, A.L. Goldberger, *Phys. Rev. E* 49 (1994) 1685.
- [12] C.-K. Peng et al., *J. Electrocardiol.* 28 (1995) 59.
- [13] A. Bunde, S. Havlin (Eds.), *Fractals and Disordered Systems*, Springer, Berlin, 1991.
- [14] A. Bunde, S. Havlin (Eds.), *Fractals in Science*, Springer, Berlin, 1994.
- [15] J. Feder, *Fractals*, Plenum Press, New York, 1988.
- [16] Y. Ashkenazy, M. Lewkowicz, J. Levitan, S. Havlin, K. Saermark, H. Moelgaard, P.E. Bloch Thomsen, *Fractals* 7 (1999) 85.
- [17] H. Moelgaard, 24-hour heart rate variability: methodology and clinical aspects, Doctoral Thesis, University of Aarhus, 1995.
- [18] H. Moelgaard, P.D. Christensen, H. Hermansen et al., *Diabetologia* 37 (1994) 788.
- [19] Y. Ashkenazy, M. Lewkowicz, J. Levitan, H. Moelgaard, P.E. Bloch Thomsen, K. Saermark, *Fractals* 6 (1998) 197.
- [20] S. Thurner, M.C. Feurstein, M.C. Teich, *Phys. Rev. Lett.* 80 (1998) 1544.
- [21] C.K. Peng, S. Havlin, H.E. Stanley, A.L. Goldberger, *Chaos* 5 (1995) 82.
- [22] L.A.N. Amaral, A.L. Goldberger, P.Ch. Ivanov, H.E. Stanley, *Phys. Rev. Lett.* 81 (1988) 2388.
- [23] P.Ch. Ivanov, L.A.N. Amaral, A.L. Goldberger, S. Havlin, M.G. Rosenblum, Z. Struzik, H.E. Stanley, *Nature* 399 (1999) 461.
- [24] T. Vicsek, *Fractal Growth Phenomena*, 2nd Edition, World Scientific, Singapore, 1993.
- [25] H. Takayasu, *Fractals in the Physical Sciences*, Manchester University Press, Manchester UK, 1997.
- [26] I. Daubechies, *Ten Lectures on Wavelets*, S.I.A.M., Philadelphia, 1992.
- [27] J.F. Muzy, E. Bacry, A. Arneodo, *Phys. Rev. Lett.* 67 (1991) 3515.
- [28] J.F. Muzy, E. Bacry, A. Arneodo, *Int. J. Bifurc. Chaos* 4 (1994) 245.